Procaine Effect on Human Erythrocyte Membrane Explored by Atomic Force Microscopy

Ulpiu Vlad Zdrenghea[1], Gheorghe Tomoaia[1], Daniela-Vasilica Pop-Toader[2], Aurora Mocanu[*,2], Ossi Horovitz[*,2] and Maria Tomoaia-Cotisel[2]

[1]*Iuliu Hatieganu University of Medicine and Pharmacy, 400132 Cluj-Napoca, Romania*

[2]*Babes-Bolyai University, Faculty of Chemistry and Chemical Engineering, 400028 Cluj-Napoca, Romania*

Abstract: The procaine effect on human erythrocytes was investigated by atomic force microscopy (AFM) at three procaine concentrations, about 5 x 10^{-7} M, 5 x 10^{-5} M and 5 x 10^{-4} M. The changes in surface morphology of erythrocyte membrane bring direct evidence on the procaine effect on the cell membrane at micro- and nanometer scale. AFM images of the control erythrocytes (without procaine) showed a well defined concave (donut) shape of cells. The structure of control erythrocytes membrane is featured by closely packed nanometer size intra-membranous particles. After the incubation of the fresh blood with increasing procaine concentrations, a progressive increase in both concave depth and surface roughness of erythrocyte membrane was observed. The particles (granules) of the membrane surface increased progressively with increasing procaine concentrations. The changes in the surface morphology of erythrocyte membrane can be associated with the enlargement of surface granules, due to the aggregation of membranous particles within the cell surface, and the domain structure formation induced by procaine. A large number of moderate elevations from 25 nm to almost 40 nm in lateral size were found to be rather uniformly distributed on the surface of whole erythrocytes at low and medium procaine concentrations, respectively. At the highest procaine concentration, the granules of about 80 nm to almost 90 nm lateral size were found to form rows rather well separated. These data are in substantial agreement with the published results obtained on membrane models in the presence of procaine.

Keywords: Erythrocyte membrane, procaine, membrane microstructure, membrane nanostructure, AFM.

INTRODUCTION

The molecular mechanism of the pharmacological action for various drugs, such as anesthetics, is mediated by membranes [1-14]. The interaction of anesthetic agents with excitable membranes is postulated to affect the specific trans-membrane proteins of the ionic channels by changing their membrane lipid micro-environment and thus, blocking the nerve signal propagation. The physiological phenomenon produced is known as anesthesia [3, 9].

Undoubtedly, the lipid phase seems to be a target for anesthetic action, being also the membrane environment in which the functional proteins are embedded. Changes induced by anesthetic agents in the organization of lipid bilayers have been reported [1-3, 5] and the anesthetic location was found to be of fundamental importance.

The Langmuir lipid monolayers [10, 11, 14-34] have been also used as an efficient model of biological membranes [11, 19, 32-34]. The anesthetics were found to expand the lipid monolayers spread at the air/water interface, at low and intermediate lateral surface pressures, depending on the pH's, ionic strengths and the surface characteristics of both the chosen lipid and anesthetic compound [10, 11, 14-33]. These arise from several possible cases, such as procaine adsorption on lipid monolayers, its binding and penetration into the lipid phase.

Changes in physical and chemical properties of lipid membrane models due to the distribution of local anesthetics within lipid membranes are believed to play an important role in the anesthetic action on natural membranes. However, the direct evidence for anesthetic, such as procaine, binding to the membrane surface of human erythrocytes has been lacking until now.

Erythrocytes have been observed by AFM [35-37], but the ultrastructure of the cell membrane network/skeleton has been not described. Isolated spectrin has also been observed by AFM [38]. A two-dimensional spectrin meshwork (network) formed by the interactions of spectrin dimers covers the entire cytoplasmic surface of the erythrocyte membrane [39, 40]. Taking advantage of AFM high sensitivity to small height variations in the surface, recently, AFM was used to image the surface of lipid membranes [24-29] and of the erythrocyte membrane [41-46], evidencing the effect of different organic or inorganic compounds on the membrane surface.

A major advantage of AFM as compared with other imaging techniques, such as SEM or optical microscopy, is that AFM provides better resolution and allows the cell membrane observation without any staining. In AFM technique, a sharp tip (radius of curvature 10-50 nm) is scanned over the cell surface at a pressing force of the order of 1-10 nN, and the height of the needle with the sharp tip is recorded at each position, thus, generating an image of the

*Address correspondence to these authors at the Babes-Bolyai University, Faculty of Chemistry and Chemical Engineering, Physical Chemistry Department, 11 Arany J. Str., 400028 Cluj-Napoca, Romania;
Tel: +40264 593833; Fax: +40264 590818;
E-mails: ossihor@yahoo.com, mocanu.aurora@gmail.com

1386-2073/11 $58.00+.00

external cell surface and of the underlying structure (external membrane skeleton) of the soft cell surface. Because the working pressing force is very low, probably the tips do not press down on the cell membrane or do not penetrate the plasma membrane and therefore, do not form images of the harder structures from inside the erythrocyte cell, such as the cytoskeleton.

There is however the possibility, that the structure of plasma membrane (containing lipid membrane with its structures near the plasma membrane, such as the membrane skeleton) could be visualized on the external (extra-cellular) surface of the plasma membrane. The goal of our research work is to examine this possibility and to develop an AFM method for observing the membrane surface at the extra cellular surface of the erythrocyte cell. We try to establish a method for studying the membrane surface of human erythrocytes by AFM, without removing the plasma membrane by detergent treatment, without staining the membrane skeleton, or by freeze/freeze-drying technique to create human red cell ghosts.

In this work, the AFM is used to observe the changes in the surface morphology of human erythrocyte membrane exposed to various procaine hydrochloride (procaine) concentrations. We have chosen the fresh human blood which is recognized to offer stable erythrocytes [42, 45] and procaine (4-amino benzoic acid [2-(diethyl amino) ethyl] ester). Procaine is a local anesthetic that contains a primary amine linked to an aromatic ring and a tertiary amine group (Scheme **1**). Consequently, it may exist as a neutral molecule, a monocation or a dication species depending on the pH values.

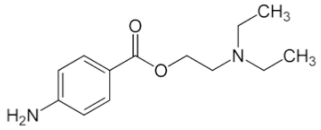

Scheme 1. Structural formula of procaine.

Previously, we reported data about acid-base equilibria for procaine in the bulk aqueous solutions and in its adsorbed layers at the fluid interfaces [47, 48]. Under physiological conditions, the calculations show that procaine is found predominantly in its monocation form but a small percentage of neutral molecules still exist.

THE ERYTHROCYTE CELL MORPHOLOGY

We used drying sessile drops on glass surface for studying the self-assembly of erythrocytes on glass from aqueous saline medium (blood diluted 1:1 v/v with salt aqueous solution at physiological concentrations of about 0.15 M NaCl) and from blood diluted 1:1 v/v with pure two distilled water. The self-organization is initiated when the sessile drop is attached to the substrate surface. The attachment leads to the appearance of a hydrodynamic centrifugal force flow that carries the colloidal phase to the drop periphery. Due to the centrifugal flow a cell ring forms at the drop edge. It becomes solid while the core of the drop is a semi-liquid gel. Latter on, salt crystallization begins in this gel matrix. Time intervals may vary depending on environmental temperature and humidity, but the sequence of events, as well as the final morphological picture of red cells, is rather stable and well reproducible. After, 2-3 days of drying up, covered with a bicker to avoid dust, water film evaporates, and additional circles arise over the middle part of the drop. Our results are similar with the reported findings [50] on the drying sessile drops for studying the self-assembly of proteins on glass from protein salt aqueous solutions.

All samples of glass supported erythrocytes without or mixed with procaine are investigated by AFM at room temperature in air. From AFM images, the direct evidence of the procaine effect on the cell membrane surface is observed at the micro- and nanometer scale.

The AFM images of the whole cell surface of the control blood sample without procaine are given in Fig. (**1**), for 10 μm x 10 μm scanned area. This figure shows that the erythrocyte cell supported by glass is rather well separated from other cells. Further, the AFM images indicate a concave (donut) shape of erythrocyte (Fig. **1a-d**) with about 8 μm in average lateral size and nearly 0.14 μm in average depth (Fig. **1** and Table **1**) of the concave shape in substantial agreement with other published data [45]. In addition, in this investigation the phase image (Fig. **1b**), the amplitude image (Fig. **1c**) and the 3D- topography (Fig. **1d**) are given beside 2D-topography (also given in [45]), to better visualize the shape of the whole erythrocyte cell and its membrane structure.

In Fig. (**2**), the nanostructure of membrane surface of control sample is given for scanned area of 500 nm x 500 nm. The nanostructure of normal human erythrocytes is featured by closely packed granules or membranous particles (Fig. **2a-d**), rather homogeneous, in round shape (Fig. **2a-c**), with average lateral size of about 22 nm (Fig. **2e**). They are almost uniformly distributed forming a surface network.

Besides using the cross section profile, as in Fig. (**1e**, or **2e**), in order to analyze the surface data from AFM images, we can characterize the roughness of the surface by the root–mean–square (RMS) value of the height distribution:

$$\mathrm{RMS} = \sqrt{\sum_{i=1}^{N} \frac{(z_i - z_m)^2}{(N-1)}}$$

where z_i is the height of i^{th} point, z_m - the mean height and N is the total number of data points in the scanned area [51, 52]. By definition, this surface roughness is a morphology-related parameter.

The roughness given by route mean square (RMS) values is very low for this sample (Table **1**), presumably reflecting that the membrane lipid molecules were imaged by AFM. Therefore, it is most likely that the lipid membrane structure of erythrocytes is visualized and it is similar with other reported data [28, 29, 43] under appropriate conditions.

The surface granules probably correspond to the aggregates of membrane lipids well packed into the lipid part of the membrane surface in substantial agreement with lipid nanostructure found in monolayer membrane models [28, 29, 49]. These particles might also correspond to membrane protein protruding from the cell surface [45].

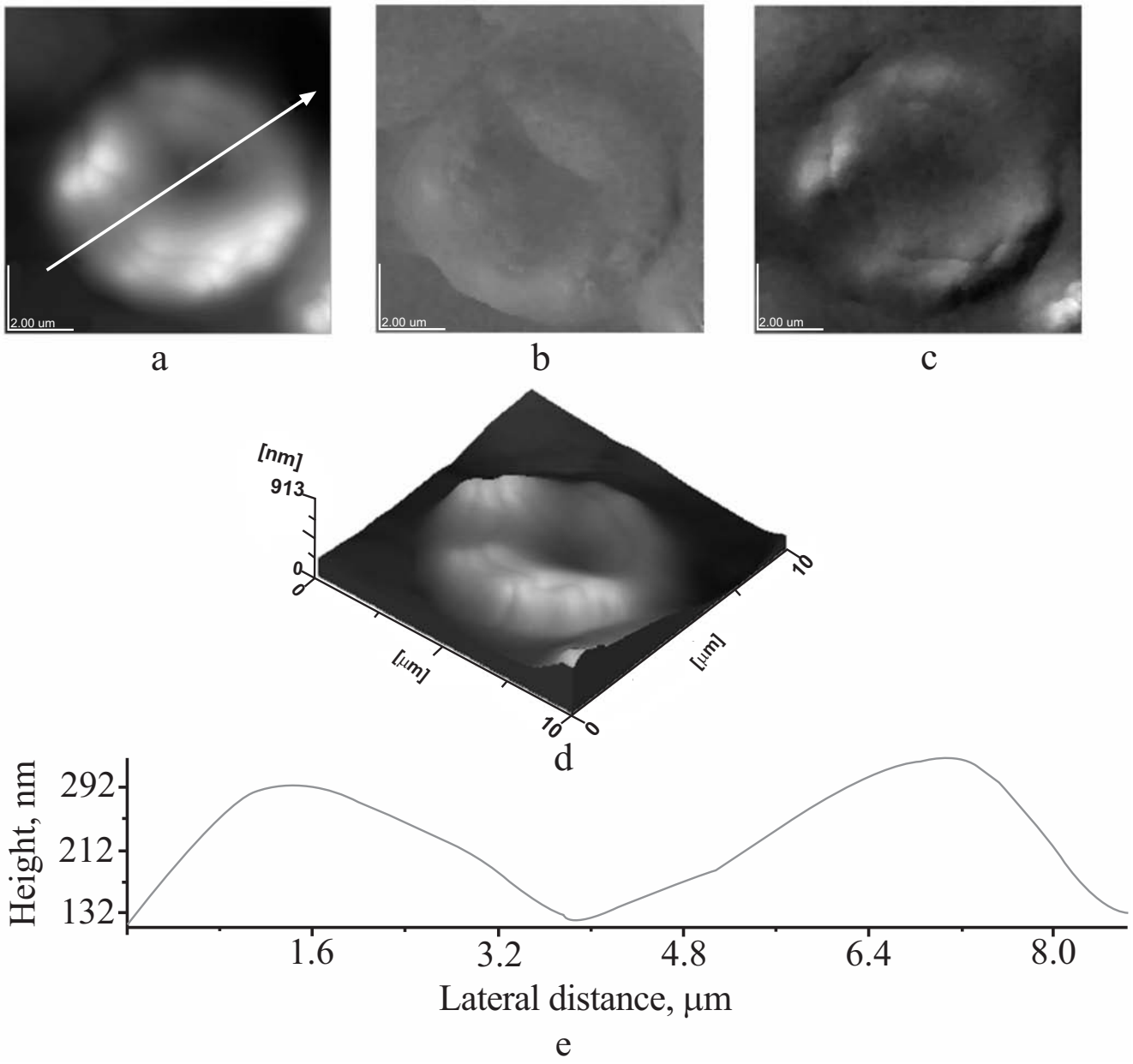

Fig. (1). AFM images of erythrocyte membrane surface, control sample. (**a**) 2D – topography; (**b**) phase image; (**c**) amplitude image; (**d**) 3D-topography; (**e**) profile of the cross section along the arrow in image (**a**). Scanned area: 10 μm x 10 μm.

THE ERYTHROCYTE CELL MORPHOLOGY IN PRESENCE OF LOW PROCAINE CONCENTRATION

Figs. (**3**, **4**) show AFM images of erythrocytes treated with low procaine concentration (5 x 10^{-7} M) for two different scanned areas. The whole surface of erythrocyte is mainly characterized by the same (donut) cell shape as for control sample without procaine in Fig. (**1**). The lateral size of the whole cell is about 8.0 μm (Table **1**). The concave deepness (about 180 or 190 nm, Table **1**) is slightly increased in comparison with that for control sample (about 140 nm or 160 nm).

The membrane nanostructure in the presence of a low procaine concentration (Fig. **4** and Table **1**) is similar (granule size of 25 nm) with that corresponding to the control sample (Fig. **2**). In addition, the surface roughness, given by root mean square (RMS), is very similar with the control sample for the same scanned area (Table **1**).

THE ERYTHROCYTE CELL MORPHOLOGY IN PRESENCE OF PROCAINE MEDIUM CONCENTRATION

The erythrocyte surface morphology is illustrated in Figs. (**5**, **6**), for two different scanned areas, at a medium concentration in procaine of 5 x 10^{-5} M. AFM images indicate an intact donut cell shape (Fig. **5a-d**) with well defined contour. Thus, AFM images show that erythrocytes are of the same concave shape as for control sample (Fig. **1**) or for erythrocytes at low procaine concentration (Fig. **3**). The concave depth is rather higher, from about 240 nm to 260 nm. The lateral size of the cell is about 8.3 or 8.1 μm (Table **1**).

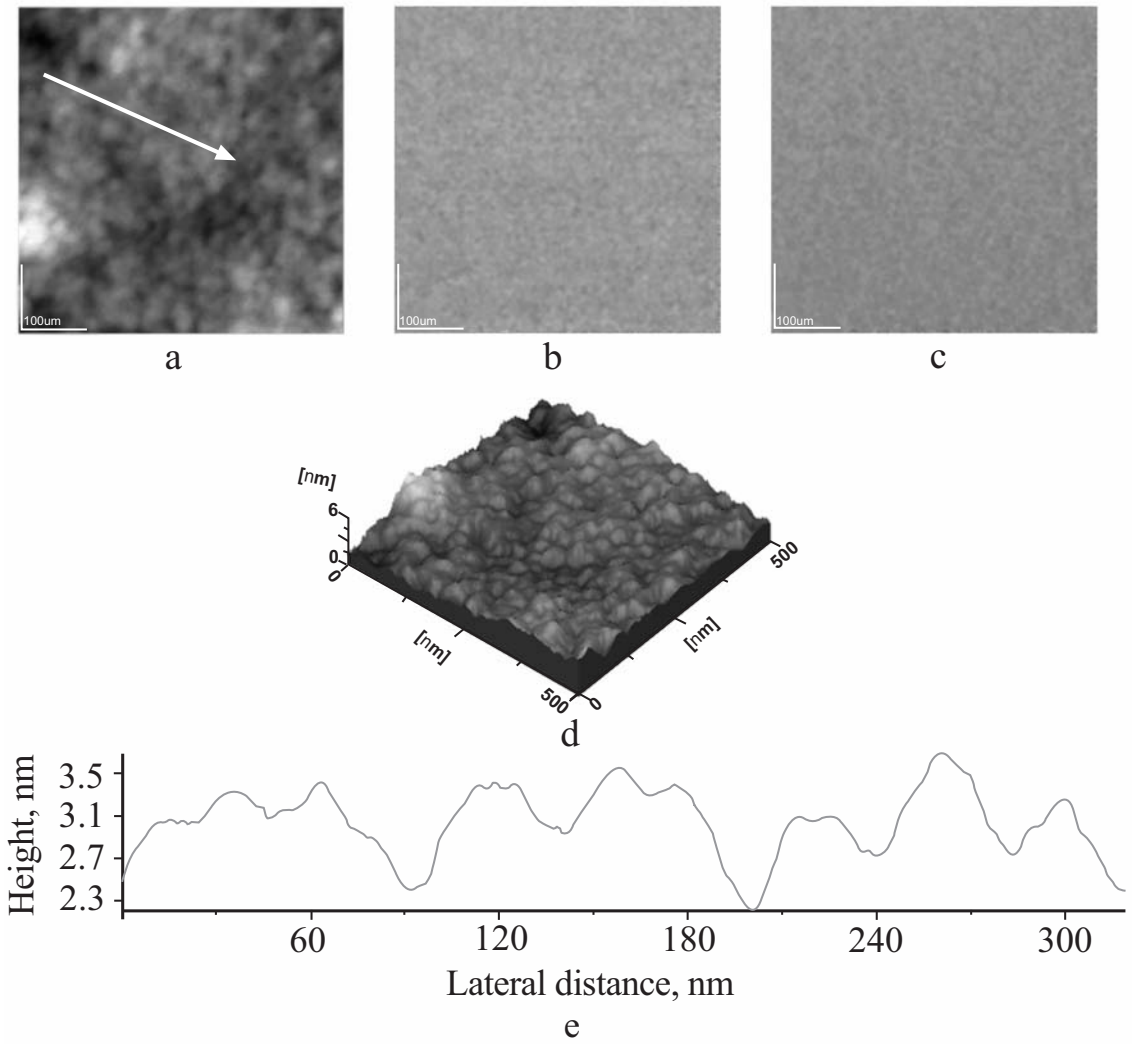

Fig. (2). AFM images of erythrocyte membrane surface, control sample as in Fig. (**1**). (**a**) 2D – topography; (**b**) phase image; (**c**) amplitude image; (**d**) 3D-topography; (**e**) profile of the cross section along the arrow in image (**a**). Scanned area: 0.5 μm x 0.5 μm.

Table 1. Erythrocytes Size, Concave Depth, Granules Lateral Size, RMS on Scanned Areas and on Cross Profile Through the Erythrocyte Membrane, for Fresh Blood Diluted with 0.15 M NaCl Solution in the 1:1 (v:v) Ratio, Without Procaine and with Three Different Concentrations of Procaine

Procaine Concentration, M	Fig.	Scanned Areas, μm x μm	Cell Size, μm	Concave Depth, nm	Granule Size, nm	RMS Scanned Areas, nm	RMS, Cross Profile, nm
0	1	10 x 10	8.0	140	-	147.0	99.0
	-	0.5x 0.5	-	-	22	0.7	0.2
	-	10 x 10	7.8	160	-	150.0	101.0
	-	1 x 1	-	-	24	0.9	0.3
	2	0.5 x 0.5	-	-	22	0.8	0.2
5×10^{-7}	3	10 x 10	8.1	180	-	167.0	81.0
	-	10 x 10	8.0	190	-	160.0	105.0
	-	1 x 1	-	-	30	1.0	0.4
	4	0.5 x 0.5	-	-	25	0.6	0.3
5×10^{-5}	5	10 x 10	8.3	240	-	175.0	108.0
	-	10 x 10	8.1	260	-	180.0	109.0
	-	1 x 1	-	-	40	3.0	0.6
	6	0.5 x 0.5	-	-	40	2.5	0.6
5×10^{-4}	7	10 x 10	8.5	766	-	256.0	267.0
	-	10 x 10	8.4	700	-	270.0	268.0
	-	1 x 1	-	-	90	10.3	2.6
	8	0.5 x 0.5	-	-	80	9.0	2.0
	-	0.5 x 0.5	-	-	90	8.0	2.0

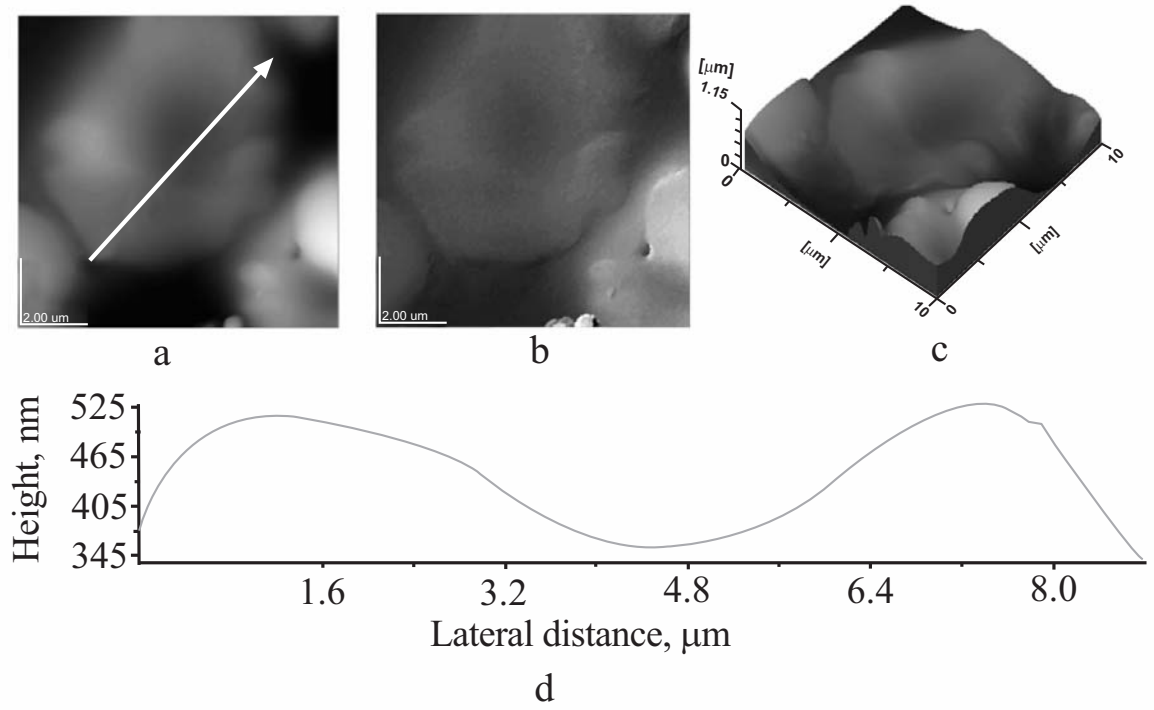

Fig. (3). AFM images of erythrocyte membrane surface in the presence of 5 x 10^{-7} M procaine. (**a**) 2D – topography; (**b**) amplitude image; (**c**) 3D-topography; (**d**) profile of the cross section along the arrow in image (**a**). Scanned area: 10 μm x 10 μm.

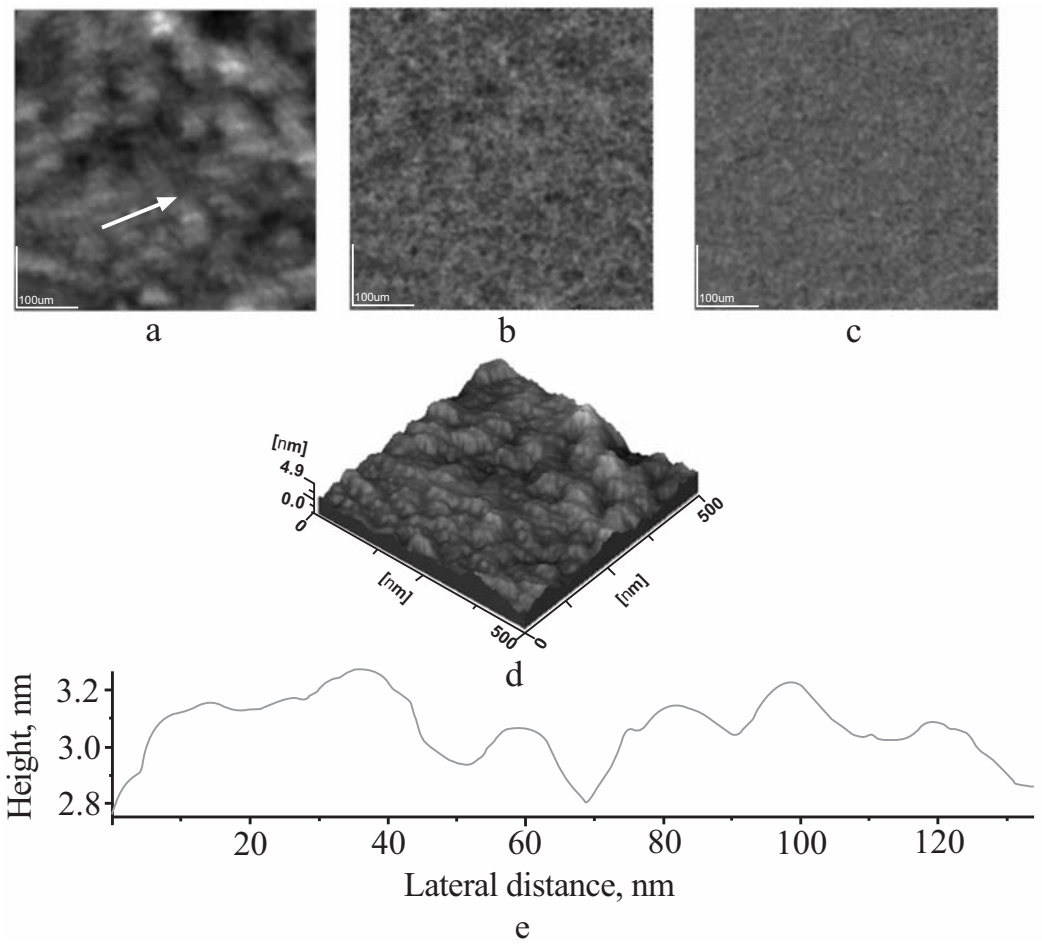

Fig. (4). AFM images of erythrocyte membrane surface in the presence of 5 x 10^{-7} M procaine as in Fig. (**3**). (**a**) 2D – topography; (**b**) phase image; (**c**) amplitude image; (**d**) 3D-topography; (**e**) profile of the cross section along the arrow in image (**a**). Scanned area: 0.5 μm x 0.5 μm.

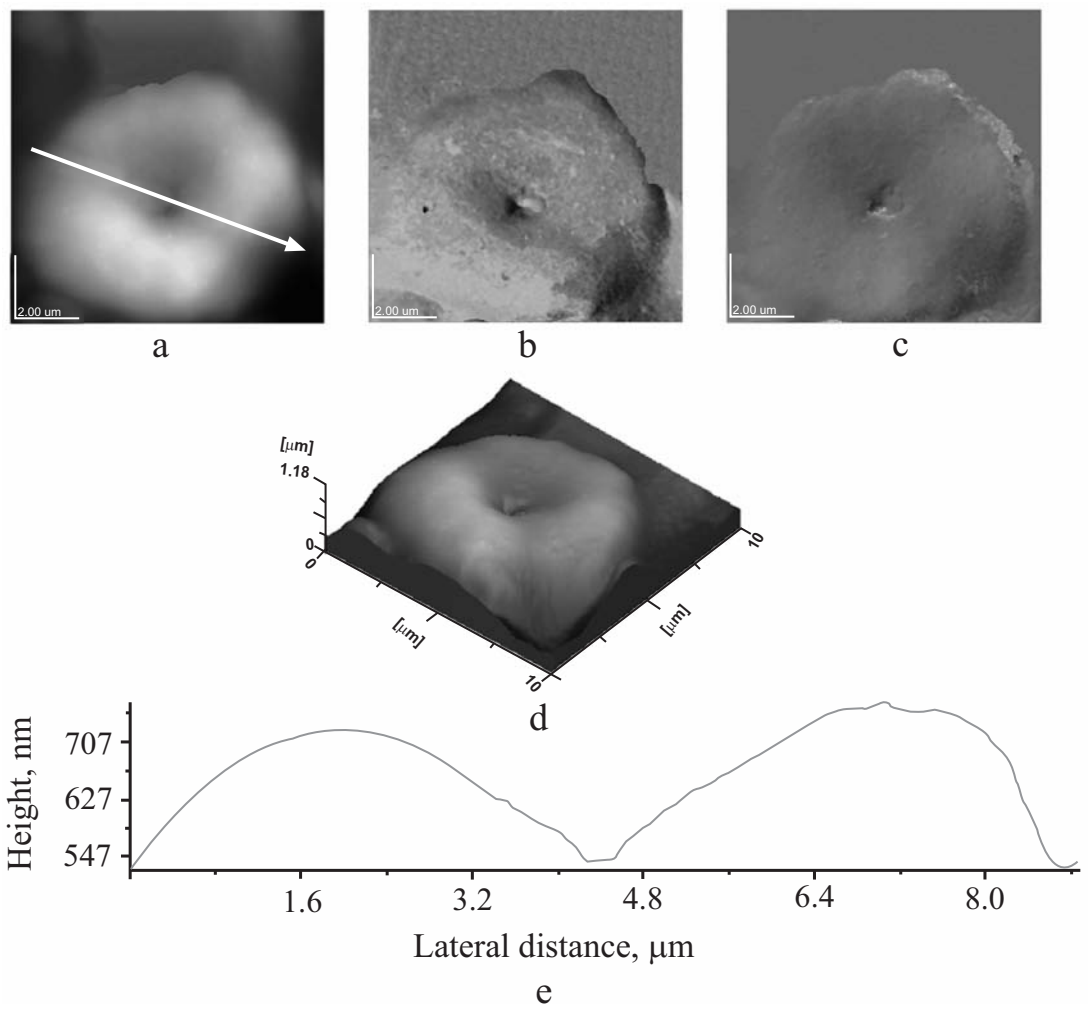

Fig. (5). AFM images of erythrocyte membrane surface in the presence of 5 x 10^{-5} M procaine. (**a**) 2D – topography; (**b**) phase image; (**c**) amplitude image; (**d**) 3D-topography, e) profile of the cross section along the arrow in image (**a**). Scanned area: 10 µm x 10 µm.

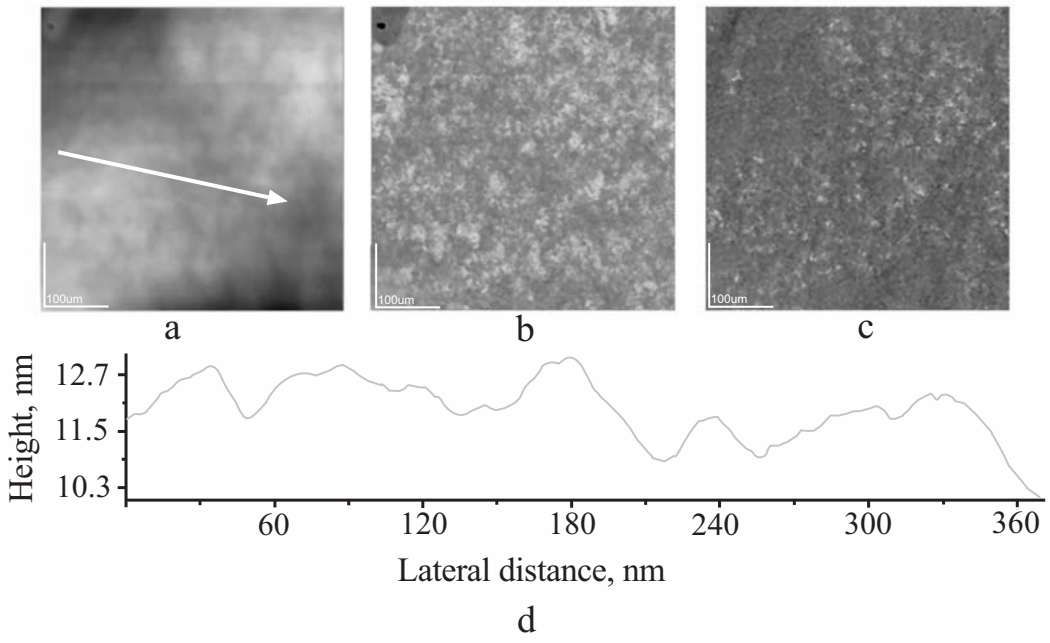

Fig. (6). AFM images of erythrocyte membrane surface in the presence of 5 x 10^{-5} M procaine as in Fig. (**5**). (**a**) 2D – topography; (**b**) phase image; (**c**) amplitude image; (**d**) profile of the cross section along the arrow in image (**a**). Scanned area: 0.5 µm x 0.5 µm.

Thus, the membrane nanostructure in the presence of a medium procaine concentration (Fig. **6**) is rather perturbed; the granules are bigger (about 40 nm lateral size) when they are compared to the corresponding ones for the control sample (Fig. **2**) or for the erythrocytes at low procaine concentration (Fig. **4**).

THE ERYTHROCYTE CELL MORPHOLOGY IN PRESENCE OF HIGH PROCAINE CONCENTRATION

The erythrocyte morphology is illustrated in Figs. (**7**, **8**), for two different scanned areas, at high procaine concentration of 5 x 10^{-4} M. AFM images indicate again an intact concave cell shape (Fig. **7a-d**), with rather well defined contour, but the cross section (Fig. **7e**) is asymmetric with a high deepness from about 700 nm up to 766 nm, much higher than for control (Fig. (**1**), or for low procaine concentration (Fig. **3d**) or even for medium procaine concentration (Fig. **5d**)), where the cross sections were almost symmetric. The lateral size of the cell is about 8.4 μm or 8.5 μm for the highest used procaine concentration (Table **1**).

The membrane nanostructure in the presence of high procaine concentration - Fig. (**8**) - is much different than the corresponding one for the control sample (Fig. **2**) or for erythrocytes in presence of low (Fig. **4**) or medium procaine concentrations (Fig. **6**). In addition, the surface roughness, given by root mean square, RMS, is the highest from the investigated cases and the granules or surface particles are larger to about 80 nm or even 90 nm (Table **1**).

DISCUSSION AND CONCLUSIONS

Increased Membrane Stability and the Domains Formation on the Cell Surface Induced by Procaine

The AFM images showed that the procaine binding to erythrocytes maintains the intact concave shape of the whole cell membrane leading to a progressive increase in membrane concave depth, in surface roughness of erythrocyte membrane and in lateral size of particles (granules) within the membrane surface with the increasing of procaine concentrations (Table **1**).

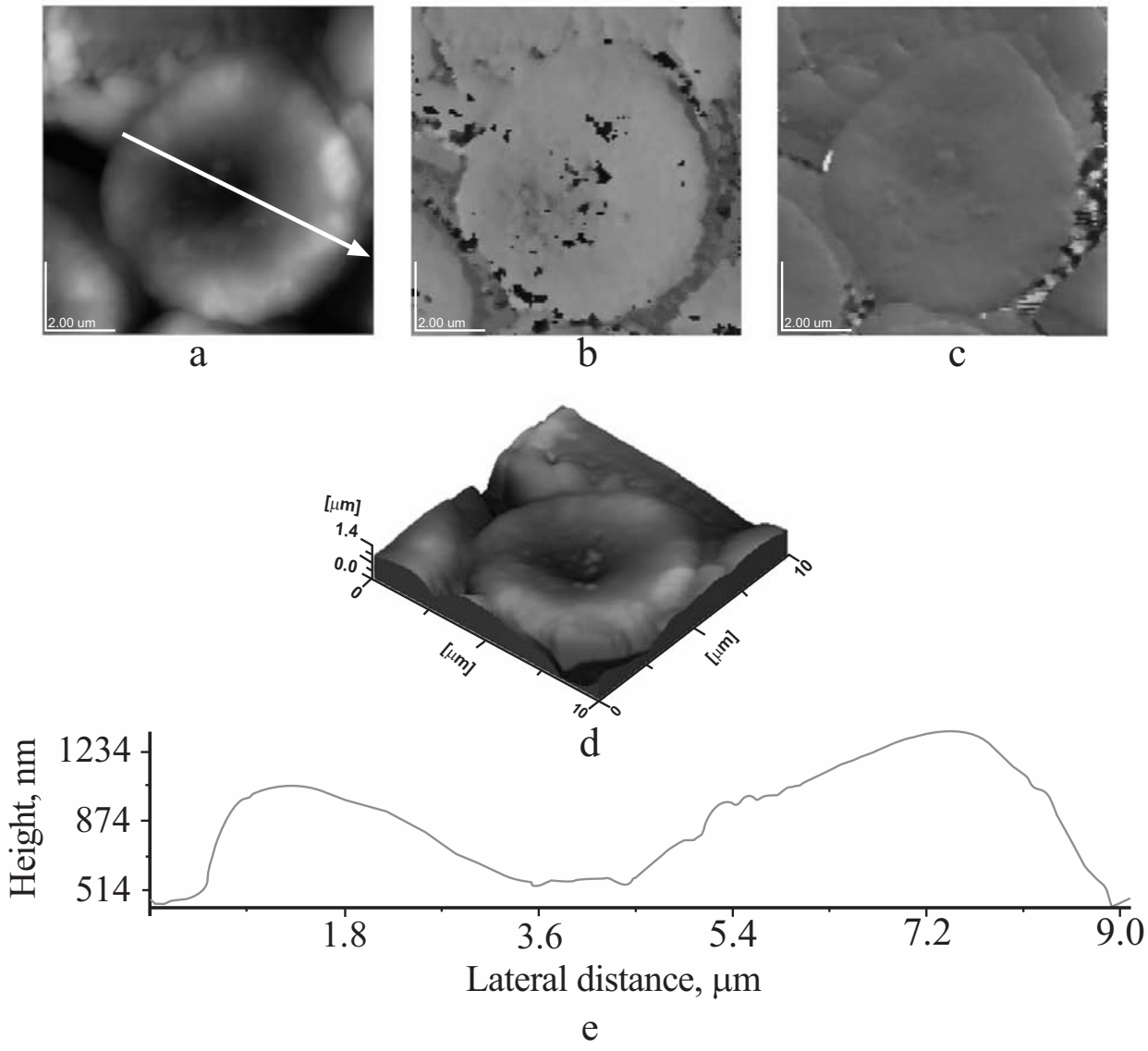

Fig. (7). AFM images of erythrocyte membrane surface in the presence of 5 x 10^{-4} M procaine. (**a**) 2D – topography; (**b**) phase image; (**c**) amplitude image; (**d**) 3D-topography; e) profile of the cross section along the arrow in image (**a**). Scanned area: 10 μm x 10 μm.

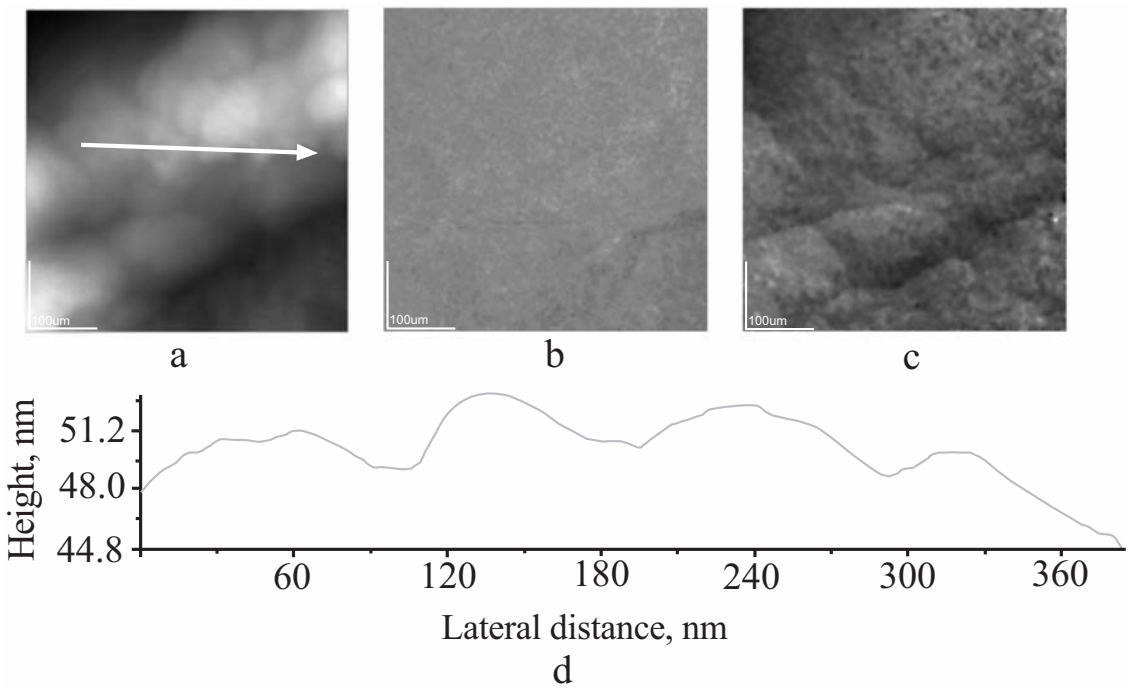

Fig. (8). AFM images of erythrocyte membrane surface in the presence of 5 x 10^{-4} M procaine as in Fig. (**7**)**.** (**a**) 2D – topography; (**b**) phase image; (**c**) amplitude image; (**d**) profile of the cross section along the arrow in image (**a**). Scanned area: 0.5 μm x 0.5 μm.

At very low procaine concentration (5 x10^{-7} M), both the morphology of erythrocytes and their nanostructures reveal no a significant difference in comparison with that situation of the control sample.

On the other hand, the AFM images showed that procaine molecules interact with erythrocytes leading progressively to the nanostructured domain formation (Table **1**) from low procaine concentration with membranous particles of average size of about 25 nm (Fig. **4e**) to medium concentration with average lateral size of granules of about 40 nm (Fig. **6e**) and mainly for high procaine concentration (Fig. **8e**), where the granules reached an average size of 80 or even 90 nm. The surface domains are formed by bigger particles, mainly at the highest used procaine concentration (5 x 10^{-4} M, Fig. **8e**).

We investigated the samples at different drying times, and it appears that the cell morphology (even evaluated in the second day after its preparation, by AFM imaging) is not dramatically distorted. Therefore, the increased height of red blood cells in the presence of high procaine concentration estimated by AFM images acquired under a well defined experimental protocol (see *Materials and Methods* section), is primarily due to the changes in the membrane properties, caused by the adsorption of procaine on the membrane surface coupled with its penetration into the plasma membrane (containing the lipid bilayer) and with its interactions with plasma membrane components. These data are in substantial agreement with the results obtained on membrane models, lipid monolayers or lipid bilayers, in intersection with procaine. From adsorption studies, Seeman [53] indicated that the local anesthetics, at comparable concentrations of anesthetic as used in our investigation, cause the expansion of the erythrocyte membrane with an intra membrane location of about 10^8 molecules of anesthetics per cell.

By comparing the nanostructures obtained by AFM with those corresponding to mixed lipid and procaine monolayers [28, 29], we can suggest that the observed structures on erythrocytes seem to correspond at least in a first approximation to the lipid part of the cell surface. The domain formation induced by procaine might thus be discussed in the first approximation on the basis of the aggregation of membrane lipids and the coexistence of different phases of membrane lipids similar with the situation of the gadolinium effect on human erythrocyte membrane [42].

Based on these findings, we suggest that procaine binds to human erythrocyte membranes and increases the membrane stability preserving the cell shape at all investigated procaine concentrations. Procaine is an anesthetic lipophilic drug, therefore probably it primarily interacts with the lipid part of the plasma membrane, presumably lipid granules, but its interaction with the glycocalix or with peripheral proteins can not be ruled out.

Evidently, the changes in the lipid layer of the erythrocyte membranes will cause the structural modifications of both internal and external proteins of the erythrocyte membranes leading to the complex self-assembly formation. Consequently, procaine might influence the interaction among lipids and proteins and might bring important changes in the whole membrane structure in substantial agreement with the results on procaine effect on lipid membrane models [28, 29].

The penetration of procaine into the lipid layers might be another cause through which procaine can also alter the interaction of lipids and proteins within erythrocyte

membrane, inducing the lipid domain formation as an effect of procaine binding to the human erythrocytes surface. The penetrated procaine into the lipid membrane can affect further the membrane ability to change.

The domain formation induced by procaine might be discussed on the basis of specific interactions among procaine and lipids in substantial agreement with the previous results obtained on model membranes, e.g., lipid monolayers [21, 22, 28, 29, 30-34, 49]. These molecular interactions lead to the aggregation of membrane components and to the coexistence of different lipids and proteins phases within erythrocyte membranes.

The increased surface pressure recorded within lipid monolayers in the presence of procaine, at comparable procaine concentrations [21, 22] as in this work, could be another reason for an increased stability of erythrocytes membrane and for changes of membrane morphology of human erythrocytes induced by procaine.

Under physiological working conditions, procaine molecule possesses the positively charged NH_3^+ group. The interplay of multiple noncovalent bonds, based on electrostatic and van der Waals interactions and on the hydrogen bonds, as well as the hydrophobic interactions are the basis for the highly specific interactions between procaine and cell membrane components that can bring changes in the membrane structure and still maintain an increased membrane stability. The notable procaine effect on cell membrane might play an important role in anesthesia and in its function as a stimulant of the nervous system.

MATERIALS AND METHODS

Procaine hydrochloride of high purity and NaCl pro analysis were purchased from Sigma Chemical Co., St. Louis, US. The procaine concentration range was from 5 x 10^{-7} to 5 x 10^{-4} M in aqueous solutions containing 0.15 M NaCl. Glass plates were purchased from Chance (Warley, UK)

Fresh human blood was used in all experiments. It was obtained from a healthy adult woman donor - one of the authors (non-smoker, type AB, Rh+). In order to avoid osmotic pressure modifications and consequently, the swelling of human blood cells, all used aqueous solutions with or without procaine contained 0.15 M NaCl.

Therefore, freshly collected finger-tip blood was diluted with 0.15 M NaCl aqueous solution in the 1:1 volume ratio, resulting in the control dispersion. The human blood was also mixed with various procaine solutions, containing 0.15 M NaCl, in the same 1:1 volume ratio as for the control dispersion. The fresh diluted blood was incubated with or without procaine, at room temperature (22 ±2^{o}C), for 30 min.

Then, 10 μL of control blood dispersion or of mixed dispersion of blood and procaine was independently deposited and adsorbed on the glass plate surface (previously optically polished). The residual dispersion was removed with a piece of filter paper and the samples were dried in the environmental air conditions. During the drying process, the control sample and the samples of blood mixed with procaine were covered with a bicker to avoid dust.

A variety of drying methods on solid supports were examined to determine the optimized conditions for the preparation of erythrocyte samples for AFM observations. To evaluate the drying effect on AFM images, the deposition and adsorption of erythrocytes on glass surface and the drying time elapsed were examined. We found that the adsorption of erythrocytes on glass surface, followed by a slightly drying period from 30 min up to 1 h, was a quite fast and straightforward method to obtain good results by AFM observations.

The dried control samples (without procaine) and those of mixed blood and procaine were imaged by atomic force microscope, AFM, JEOL 4210. The silicon cantilevers (spring constant 11.5 N m^{-1}, nominal tip radius 10 nm, resonance frequency of 250 – 350 kHz) were used. For AFM examination, five fresh samples of glass supported erythrocytes were obtained from each blood dispersion, prepared without or with procaine. Then, at least four macroscopically separate areas were imaged for every sample. Through this investigation, AFM images were obtained at several procaine concentrations in order to examine the effect of procaine on erythrocyte membrane. The experimental details on AFM, operating in tapping (semi-contact) mode, are given elsewhere [24-29].

Because the fresh blood samples were used for each experiment the anticoagulant compound was not used. However, we tried experiments in the presence of anticoagulant agent, such as trypsin, but the self assembled erythrocytes arrangements on glass obtained in the presence of anticoagulant were similar those in the absence of coagulant. The resolution of AFM images was better in the absence of anticoagulant agent.

ACKNOWLEDGEMENTS

This work was supported by the research project no. 41-050/2007.

REFERENCES

[1] Tsuchiya, H.; Mizogami, M.; Ueno, T.; Takakura, K. Interaction of local anaesthetics with lipid membranes under inflammatory acidic conditions. *Inflammopharmacol*., **2007**, *15*, 164-170.

[2] Leonenko, Z.; Finot, E.; Cramb, D. AFM study of interaction forces in supported planar DPPC bilayers in the presence of general anesthetic halothane. *Biochim. Biophys. Acta*, **2006**, *1758*, 487-492.

[3] Leonenko, Z. V.; Cramb, D. T. Revisiting lipid-general anesthetic interactions (I): Thinned domain formation in supported planar bilayers induced by halothane and ethanol. *Can. J. Chem*., **2004**, *82*, 1128-1138.

[4] Tomoaia-Cotisel, M.; Tomoaia, G.; Zsako, I.; Mocanu, A.; Albu, I. The influence of the local anesthetic procaine on phospholipid membranes. Some implications in anesthesia. *J. Colloid. Surface Chem*., **2001**, *4*(1), 13-25.

[5] Hata, T.; Matsuki, H.; Kaneshina, S. Effect of local anesthetics on the phase transition temperatures of ether- and ester-linked phospholipid bilayer membranes. *Colloids Surf. B*., **2000**, *18*, 41-50.

[6] Zsako, J.; Tomoaia-Cotisel, M.; Mocanu, A. Interaction of procaine with biomembranes. *Stud. Univ. Babeş-Bolyai, Chem*., **2000**, *45*(1-2), 175-183.

[7] Matsuki, H.; Kaneshina, S.; Kamaya, H.; Ueda, I. Partitioning of charged local anesthetics into model membranes formed by cationic surfactant: Effect of hydrophobicity of local anesthetic molecules. *J. Phys. Chem. B*, **1998**, *102*, 3295-3304.

[8] Barbinta-Patrascu, M. E.; Tugulea, L.; Meghea, A. Procaine effects on model membranes with chlorophyll A. *Rev. Chim. (Bucharest)*, **2009**, *60*, 337-341.

[9] Bondar, A. N.; Suhai, S.; Smith, J. C.; Frangopol, P.T. Computer simulations of local anesthetics mechanism: Quantum chemical investigation of procaine. *Romanian Reports in Physics*, **2007**, *59* (2), 289-299.

[10] Tomoaia-Cotisel, M. On the mechanism of procaine penetration into stearic acid monolayers spread at the air/water interface. *Prog. Colloid Polym. Sci.*, **1990**, *83*, 155-166.

[11] Asgharian, B.; Cadenhead, D. A.; Tomoaia-Cotisel, M. An epifluorescent microscopy study of the effects of procaine on model membrane systems. *Langmuir*, **1993**, *9*, 228-232.

[12] Hianik T.; Fajkus, M.; Tarus, B.; Frangopol, P. T.; Markin, V. S.; Landers, D. F. The ellectrostriction, surface potential and capacitance relaxation of bilayer lipid membranes induced by tetracaine. *Bioelectrochem Bioenerg.*, **1998**, *46*, 1-5.

[13] Frangopol, P. T.; Mihailescu. D. Interactions of some local anesthetics and alcohols with membranes. *Colloids Surf. B.*, **2001**, *22*, 3-22.

[14] Tomoaia-Cotisel, M.; Chifu, E.; Mocanu, A.; Zsakó, J.; Salajan, M.; Frangopol, P. T. Stearic acid monolayers on procaine containing subphases. *Rev. Roum. Biochim.*, **1988**, *25*, 227-237.

[15] Tomoaia-Cotisel, M.; Zsakó, J.; Chifu, E.; Frangopol, P. T.; Luck, W. A. P.; Osawa, E. Interaction of procaine with uncharged stearic acid monolayers at the air/water interface. *Rev. Roum. Biochim.*, **1989**, *26*, 305-313.

[16] Zsakó, J.; Tomoaia-Cotisel, M.; Chifu, E.; Mocanu, A; Frangopol, P. T. Influence of stearic acid monolayers upon the procaine adsorption from underlying alkaline aqueous solutions. *Biochim. Biophys. Acta*, **1990**, *1024*, 227-232.

[17] Chifu, E.; Tomoaia-Cotisel, M.; Zsakó, J.; Albu, I.; Mocanu, A.; Frangopol, P. T. Penetration of procaine hydrochloride into stearic acid monolayers from underlying aqueous solutions. *Rev. Roum. Chim.*, **1990**, *35*, 879-889.

[18] Chifu, E.; Tomoaia-Cotisel, M.; Zsakó, J.; Mocanu, A.; Salajan, M.; Neag, M.; Frangopol, P. T. Procaine penetration into uncharged stearic acid monolayers in terms of Gibbs' adsorption equation In: *Seminars in Biophysics*, Vol. *6*, Frangopol, P.T.; Morariu, V. V., Editors, Bucharest: IAP Press, **1990**, pp. 117-128.

[19] Tomoaia-Cotisel, M.; Cadenhead, D. A. Interaction of procaine with stearic acid monolayers at the air/water interface. *Langmuir*, **1991**, *7*, 964-974.

[20] Tomoaia-Cotisel, M.; Zsakó, J.; Chifu, E.; Mocanu, A.; Frangopol, P. T.; Quinn, P. J. Procaine binding to stearic acid monolayers spread at the air/buffer interface. The influence of pH and surface pressures. *J. Rom. Colloid Surf. Chem. Assoc.*, **1997**, *2*(3-4), 30-36.

[21] Zsakó, J.; Tomoaia-Cotisel, M.; Chifu, E.; Mocanu, A.; Frangopol, P. T. Procaine interactions with phospholipid monolayers at the air/water interface. *Gazz. Chim. Ital.*, **1994**, *124*, 5-9.

[22] Zsakó, J.; Chifu, E.; Tomoaia-Cotisel, M.; Mocanu, A.; Frangopol, P. T. Procaine penetration into mixed monomolecular films of cholesterol and dipalmitoyl phosphatidylcholine. *Rev. Roum. Chim.*, **1994**, *39*, 777-786.

[23] Tomoaia-Cotisel, M.; Chifu, E.; Zsakó, J.; Frangopol, P. T.; Quinn, P. J.; Mocanu. A. Interaction of some drugs with monomolecular membranes at the fluid interfaces. *Stud. Univ. Babes-Bolyai, Chem.*, **1993**, *38*(1-2), 81-85.

[24] Tomoaia-Cotisel, M.; Tomoaia, G.; Pop, V. D.; Mocanu, A.; Cozar, O.; Apetroaei, N.; Popa, G. Atomic force microscopy studies of Langmuir-Blodgett films. The effect of some drugs on dipalmitoyl phosphatidylcholine. *Stud. Univ. Babes-Bolyai, Phys.*, **2004**, *49*(3), 141-152.

[25] Tomoaia-Cotisel, M.; Tomoaia, G.;, Pop, V. D.; Mocanu, A.; Apetroaei, N.; Popa, G. Atomic force microscopy studies of Langmuir-Blodgett films. 2. Phase behavior of stearic acid monolayers. *Rev. Roum. Chim.*, **2005**, *50*, 381-390.

[26] Tomoaia-Cotisel, M.; Tomoaia, G.; Pop, V. D.; Mocanu, A.; Cozar, O.; Apetroaei, N.; Popa, G. Atomic force microscopy studies of Langmuir-Blodgett films. 3. Phase behaviour of dipalmitoyl phosphatidyl choline monolayers. *Rev. Roum. Chim.*, **2005**, *50*, 471-478.

[27] Tomoaia-Cotisel, M.; Pop, V. D.; Tomoaia, G.; Mocanu, A.; Racz, C.; Ispas, C. R.; Pascu, O.; Borostean, O. C. Atomic force microscopy studies of Langmuir-Blodgett films. 4. The influence of aluminum substrate on dipalmitoyl phosphatidylcholine nanolayers. *Stud. Univ. Babes-Bolyai, Chem.*, **2005**, *50*(1), 23-37.

[28] Tomoaia-Cotisel, M.; Mocanu, A. Phase transitions in phospholipid monolayers studied by atomic force microscopy and Langmuir-Blodgett technique. *Rev. Chim. (Bucharest)*, **2008**, *59*, 1230-1233.

[29] Frangopol, P. T.; Cadenhead, D. A.; Tomoaia-Cotisel, M.; Mocanu, A. Procaine effects on surface topography of spread dipalmitoylphosphatidylcholine monolayers. *Studia Univ. Babes-Bolyai, Chem.*, **2009**, *54*(1), 23-35.

[30] Matsuki, H.; Shimada, K.; Kaneshina, S.; Yamanaka, M.; Kamaya, H.; Ueda, I. Exclusion of the local anesthetic procaine hydrochloride from a surface-adsorbed film and micelle of decylammonium chloride. *Langmuir*, **1997**, *13*, 6115-6119.

[31] Goodman, D. M.; Nemoto, E. M.; Evans, R. W.; Winter, P. M. *Chem.* Anesthetics modulate phospholipase C hydrolysis of monolayer phospholipids by surface pressure. *Chem. Phys. Lipids.*, **1996**, *84*, 57-64.

[32] Choi, S. Y.; Oh, S. G.; Lee, J. S. Effects of lidocaine-HCl salt and benzocaine on the expansion of lipid monolayers employed as bio-mimicking cell membrane. *Colloids Surf. B.*, **2001**, *20*, 239-244.

[33] Choi, S. Y.; Oh, S. G.; Lee, J. S. Effects of lidocaine on the expansion of lipid monolayer at air/water interface in relation to the local anesthesia. *Colloids Surf B.*, **2000**, *17*, 255-264.

[34] Cavalli, A.; Borissevitch, G.; Tabak, M.; Oliveira Jr., O. N. Interaction of dibucaine with lipids in mixed Langmuir monolayers. *Thin Solid Films*, **1996**, *284-5*, 731-734.

[35] Butt, H. J.; Wolff, E. K.; Gould, S. A. C.; Northern, B. D.; Peterson, C. M.; Hansma, P. K. Imaging cells with the atomic force microscope. *J. Struct. Biol.*, **1990**, *105*, 54-61.

[36] Han, W.; Mou, J.; Sheng, J.; Yang, J.; Shao, Z. Cryo atomic force microscopy: A new approach for biological imaging at high resolution. *Biochemistry*, **1995**, *34*, 8215-8220.

[37] Zhang, Y.; Sheng, S. J.; Shao, Z. Imaging biological structures with the cryo atomic force microscope. *Biophys. J.*, **1996**, *71*, 2168 - 2176.

[38] Almqvist, N., Backman, L.; Fredriksson, S. Imaging human erythrocyte spectrin with atomic force microscopy. *Micron*, **1994**, *25*, 227-232.

[39] Lux, S. E. Dissecting the red cell membrane skeleton. *Nature*, **1979**, *281*, 426-428.

[40] Marchesi, V. T. Stabilizing infrastructure of cell membranes. *Annu. Rev. Cell. Biol.*, **1985**, *1*, 531-561.

[41] Iwamoto, H.; Wakayama, N. Atomic force microscopy studies of erythrocyte membranes immobilized by centrifugation under aqueous conditions. *Jpn. J. Appl. Phys.*, **1997**, *36*, 3872-3876.

[42] Cheng, Y.; Liu, M.; Li, R.; Wang, C.; Bai, C.; Wang, K. Gadolinium induces domain and pore formation of human erythrocyte membrane: an atomic force microscopic study. *Biochim. Biophys. Acta –Biomembranes*, **1999**, *1421*, 249-260.

[43] Cheng, Y.; Liu, M.; Li, Y.; Li, R.; Bai, C.; Wang, K. Formation of domain structure of erythrocyte membrane in Wistar rat fed with $CeCl_3$ per os. *Chin. Sci. Bull.*, **2000**, *45*, 426-429.

[44] Yamashina, S.; Katsumata, O. Structural analysis of red blood cell membrane with an atomic force microscope. *J. Electron Microsc.*, **2000**, *49*, 445-451.

[45] Zhang, X. Y.; Chen, F. H.; Wei, P. H.; Ni, J. Z. Studies on the effects of epimedium extract on erythrocytes. *Chin. Chem. Lett.*, **2006**, *17*, 1105-1108.

[46] Ho, M. S.; Kuo, F. J.; Lee, Y. S.; Cheng, C. M. Atomic force microscopic observation of surface-supported human erythrocytes. *Appl. Phys. Lett.*, **2007**, *91*, 023901.

[47] Zsakó, J.; Tomoaia-Cotisel, M.; Chifu, E.; Albu, I.; Mocanu, A.; Frangopol, P. T. Protolytic equilibria in surface solutions of stearic acid, procaine and benzoic acid at the air/water interface. *Rev. Roum. Chim.*, **1990**, *35*, 867-877.

[48] Zsakó, J.; Tomoaia-Cotisel, M.; Albu, I.; Mocanu, A.; Chifu, E.; Frangopol, P. T. Acid-base properties of some local anesthetics. *Rev. Roum. Biochim.*, **1991**, *28*, 33-40.

[49] Makino, M.; Kamiya, M.; Nakajo, N.; Yoshikawa, K. Effects of local anesthetics on the dynamic behavior of phospholipid thin film. *Langmuir*, **1996**, *12*, 4211-4217.

[50] Yakhno, T. Salt-induced protein phase transitions in drying drops. *J. Coll. Interface Sci.* **2008**, *318*, 225-30.

[51] Girasole, M.; Pompeo, G.; Cricenti, A.; Congiu-Castellano, A.; Andreola, F.; Serafino, A.; Frazer, B. H.; Boumis, G.; Amiconi, G. Roughness of the plasma membrane as an independent

morphological parameter to study RBCs: A quantitative atomic force microscopy investigation. *Biochim. Biophys. Acta*, **2007**, *1768*, 1268-1276.

[52] Wu, Y.; Hu, Y.; Cai, J.; Ma, S.; Wang, X.; Chen, Y. The analysis of morphological distortion during AFM study of cells. *Scanning*, **2008**, *30*, 426-432.

[53] Seeman, P. Erythrocyte membrane stabilization by local anesthetics and tranquilizers. *Biochemical Pharmacology*, **1966**, *15*, 1753-62, IN1-IN2, 1763-1766.

Received: January 14, 2011 **Revised: March 2, 2011** **Accepted: March 3, 2011**